



The variety of subaerial active salt deformations in the Kuqa fold-thrust belt (China) constrained by InSAR



Cindy Colón^{a,*}, A. Alexander G. Webb^b, Cécile Lasserre^{c,d}, Marie-Pierre Doin^{c,d}, François Renard^{c,d,e}, Rowena Lohman^f, Jianghai Li^g, Patrick F. Baudoin^a

^a Department of Geology and Geophysics, Louisiana State University, Baton Rouge, LA, 70803, USA

^b Department of Earth Sciences, University of Hong Kong, Hong Kong, China

^c ISTERre, University Grenoble Alpes, BP53, 38041, Grenoble Cedex 09, France

^d ISTERre, CNRS, BP53, 38041, Grenoble Cedex 09, France

^e PGP, Dept. Geosciences, University of Oslo, Box 1048, Blindern, 0316 Oslo, Norway

^f Earth and Atmospheric Sciences, Cornell University, Ithaca, NY, 14850, USA

^g The Key Laboratory of Orogenic Belts and Crustal Evolution, Ministry of Education, School of Earth and Space Sciences, Peking University, Beijing 100871, China

ARTICLE INFO

Article history:

Received 11 December 2015

Received in revised form 8 May 2016

Accepted 9 June 2016

Available online xxx

Editor: P. Shearer

Keywords:

Kuqa fold-thrust belt

salt deformation

namakiers

InSAR

ABSTRACT

Surface salt bodies in the western Kuqa fold-thrust belt of northwestern China allow study of subaerial salt kinematics and its possible correlations with weather variations. Ephemeral subaerial salt exposure during the evolution of a salt structure can greatly impact the subsequent development and deformation of its tectonic setting. Here, we present a quantitative time-lapse survey of surface salt deformation measured from interferometric synthetic aperture radar (InSAR) using Envisat radar imagery acquired between 2003 and 2010. Time series analysis and inspection of individual interferograms confirm that the majority of the salt bodies in western Kuqa are active, with significant InSAR observable displacements at 3 of 4 structures studied in the region. Subaerial salt motion toward and away from the satellite at rates up to 5 mm/yr with respect to local references. Rainfall measurements from the Tropical Rainfall Measuring Mission (TRMM) and temperature from a local weather station are used to test the relationship between seasonality and surface salt motion. We observe decoupling between surface salt motion and seasonality and interpret these observations to indicate that regional and local structural regimes exert primary control on surface salt displacement rates.

© 2016 Elsevier B.V. All rights reserved.

1. Introduction

Analysis of subaerial salt behavior is limited because allochthonous salt outcrops are rarely preserved on the Earth's surface, making subsurface imaging the primary technique for observing salt deposits (Talbot and Pohjola, 2009). Few examples of salt bodies outcrop at the surface today (Zagros, Iran; Salt Range, Pakistan), not including submarine salt exposures. Interpretations of many subsurface salt bodies throughout the world have indicate subaerial exposure during structural evolution (e.g., Canerot et al., 2005). This subaerial exposure may be short-lived and yet have key impacts on the long-term evolution because salt bodies interacting with surface processes may display sharply distinct kinematics versus subsurface salt bodies. As a result, it is important for the overall exploration of crustal salt to study the few

available subaerial salt bodies. Many structural systems dominated by salt deformation are commonly associated with major hydrocarbon reservoirs. Additional compelling reasons to explore subaerial salt bodies are (1) distinctive mechanical properties of salt make it one of the few solid Earth materials able to flow at the surface, and (2) these represent Earth-surface deformation systems that can be highly responsive to weather conditions (Talbot and Rogers, 1980).

Much of our current understanding of surface salt kinematics stems from namakier (extrusive salt “glaciers”, also called “salt fountains”) studies predominantly in the Alborz and Zagros Mountains in northern and southern Iran, respectively (e.g., Kent, 1979). Over one hundred Hormuz salt diapirs, fed from pipe-like conduits (point-sourced), are known to exist in the Zagros Mountains (Kent, 1979). Of these salt bodies, surface motion has been observed on twenty diapirs using a satellite-based remote sensing technique called interferometry of synthetic aperture radar (InSAR) capable of measuring millimeter-scale vertical displacements (Barnhart and Lohman, 2012). The sheet-like Garmsar salt nappe of the Alborz Mountains extruded along a frontal thrust before

* Corresponding author.

E-mail address: cincolon@gmail.com (C. Colón).

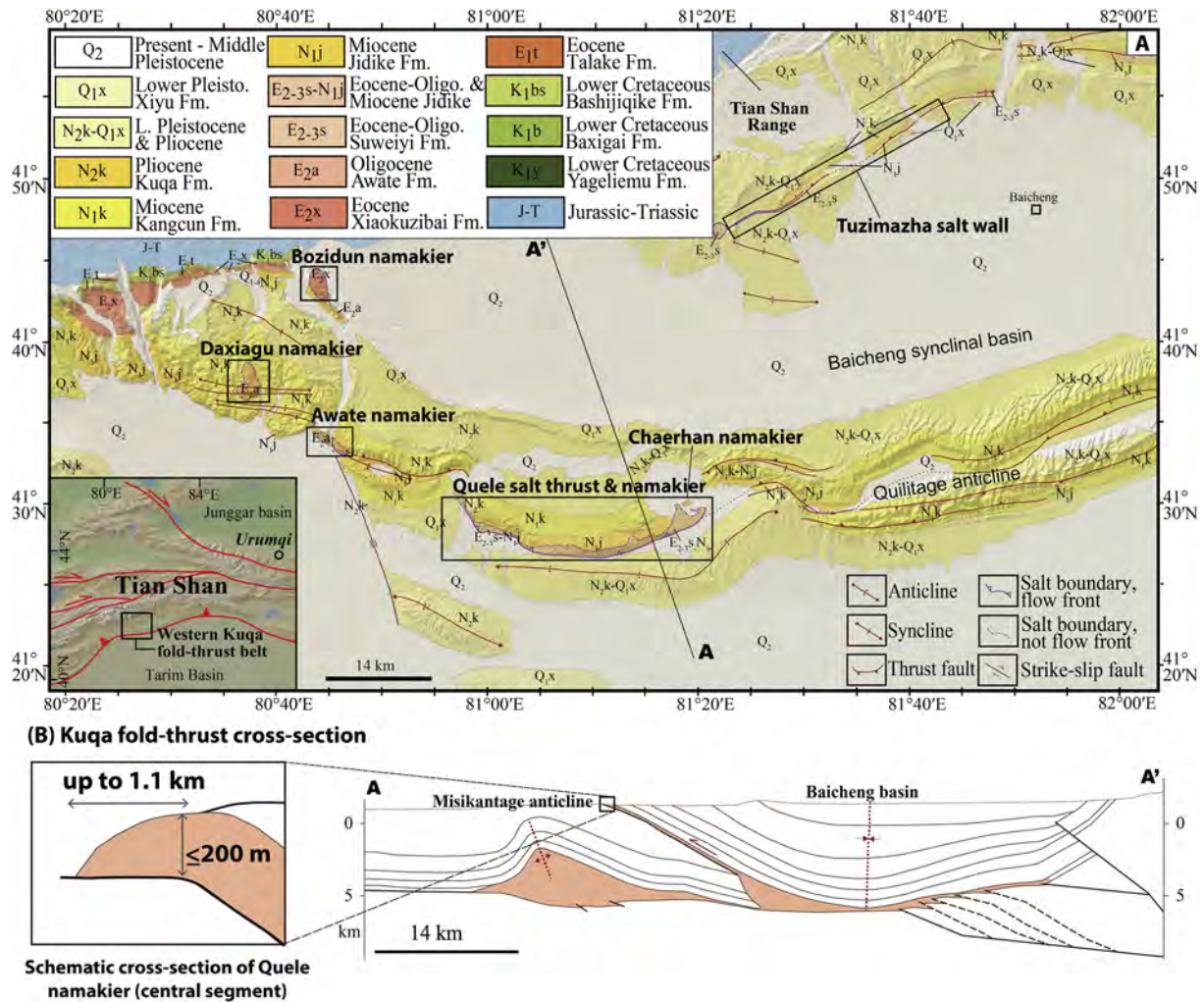


Fig. 1. (Top) Geologic map of the western Kuqa fold-thrust belt, adapted from Li et al. (2014), located south of Tian Shan Mountain Range and northern Tarim Basin. Blue and green units toward the north represent Tian Shan bedrock. Yellow and orange units represent Cenozoic basin deposits. (Bottom) Cross section (adapted from Li et al., 2012) from the southern Tian Shan through the Kuqa fold-thrust belt, toward the Tarim basin and dissects the Quele salt nappe and the Misikantage anticline. The schematic cross section of Quele namakier is more representative of the central portion of Quele namakier. (For interpretation of the references to color in this figure legend, the reader is referred to the web version of this article.)

undergoing open-toed advance and is presently inactive; the motion detected by InSAR is attributed to dissolution (Baikpour et al., 2010). Furthermore, InSAR has also been used to detect continuous vertical, upward flow rates between 5.5–8.3 mm/yr across the line-sourced Sedom diapir in the Dead Sea basin (Weinberger et al., 2006).

Recently recognized namakiers in the western Kuqa fold-thrust belt in northwestern China provide a new natural laboratory to observe and constrain subaerial salt kinematics (Li et al., 2014). Four active point-sourced namakiers exist in western Kuqa fold-thrust belt (Fig. 1). An active line-sourced diapir, the Tuzimazha salt wall, is comparable to the Sedom diapir with vertical, upward flow. Quele namakier, exposed in western Kuqa fold-thrust belt, is an active open-toed, line-sourced subaerial salt structure extruded from a surface-breaching thrust fault on Earth's surface. Kuqa fold-thrust belt provides an invaluable opportunity to study the behavior of a variety of subaerial salt bodies within the same geologic setting. Furthermore, the Kuqa fold-thrust belt is more accessible than other examples of subaerial salt extrusion like the Salt Range of Pakistan.

Existing work concludes that the presence of meteoric water and fluctuating temperatures are the principal factors enabling salt recrystallization and/or dissolution after surface extrusion (Talbot and Rogers, 1980; Urai et al., 1986; Desbois et al., 2010). In the








present study, we use InSAR to measure the spatial and temporal deformation patterns of namakiers in Kuqa fold-thrust belt. We compare these observations to rainfall and temperature measurements in order to explore potential relationships between the active surface salt kinematics and local weather conditions (Fig. 2).

2. Background

2.1. Geologic setting

The Kuqa foreland fold-thrust belt actively accommodates ~4–7 mm/yr of north–south tectonic shortening between the Tian Shan to the north and the Tarim basin to the south across a ~400 km long, ~20–65 km wide region (e.g., Allen et al., 1991). Contractual tectonics have formed structural hydrocarbon traps across Kuqa fold-thrust belt where the deformational style is controlled by the presence and varying thickness of salt layers (e.g. Tang et al., 2004; Chen et al., 2004). The subsalt sequence (Upper Permian–Cretaceous) includes Triassic–Jurassic coal and lacustrine mudstones that matured into regional hydrocarbon source rocks (Hendrix et al., 1992; Tang et al., 2004; Chen et al., 2004). Two salt dominated units control deformation across Kuqa (Li et al., 2012): the Miocene Jidike Formation and Paleocene–Eocene Kumugeliemu Group concentrated in east-

Factors impacting subaerial salt structure motion

Variable	Temporal range	Spatial flow range	Kinematic response to external condition
Hot (surface temp.)	hourly, daily, seasonal	<mm to cm	 Thermal expansion may cause inflation and overall relative surface uplift of the namakier when surface temperatures are high
Cold (surface temp.)	hourly, daily, seasonal	<mm to cm	 Thermal contraction may cause deflation and overall relative surface subsidence of the namakier when temperatures are low
Wetness	daily, seasonal	<mm to meters	 Meteoric waters facilitates pressure-solution GBS which accelerates salt flow. As salt spreads faster and further laterally, the namakier's surface appears to subside
Dryness (a)	seasonal	<mm to cm	 Dry-inflation scenario suggests the carapace, developed during dry periods, inhibits lateral spreading and facilitates swelling above the orifice resulting in relative surface uplift above the orifice
Dryness (b)	seasonal	<mm to cm	 Dry-deflation scenario suggests the carapace, developed during dry periods, hinders uplift of the central dome and promotes lateral spreading resulting in surface subsidence of the namakier as it spreads laterally
Thin Overburden	seasonal, annually	<mm to cm	 If enough material is removed from the top of a namakier, thereby reducing the overburden above the orifice, and causing an increase salt extrusion rate which results in surface uplift above the orifice
Thick Overburden	>annually	<mm to cm	 If a namakier carapace thickens significantly then the additional load from may cause enough resistance to decrease the salt extrusion rate resulting in reduced namakier growth

↓ = vertical surface motion ↗ = dominant salt flow direction

Fig. 2. Chart highlights variables that may control subaerial salt motion, their temporal and spatial ranges, and an illustration and description of the predicted kinematic impact. White arrows represent dominant salt flow direction. Black arrows represent surface displacement direction. Swelling of the salt in hot weather due to thermal expansion and deflation during cold weather because of thermal contraction may occur however the range of motion may be very small. During and shortly after rainfall events surface salt flow is predicted to accelerate significantly albeit short lived. During dry periods, 2 opposing models explain surface salt behavior: Dryness (a) predicts the strong carapace that develops during dry periods inhibits lateral spreading and facilitates swelling at the dome (above the orifice) as the salt extrudes from the feeder. Dryness (b) predicts that the thick carapace hinders uplift of the central dome and instead promotes lateral spreading. The presence of a thin weak overburden/carapace can potentially reduce overburden stress and accelerate salt extrusion. A thick, strong overburden/carapace may apply enough overburden stress to reduce salt extrusion rates.

ern and western Kuqa, respectively. The Kumugeliemu Group consists of halite and gypsum interbedded with mudstone, sandstone, conglomerate and marl (Hendrix et al., 1992; Chen et al., 2004). These strata had an original thickness of ~1100 m and the range of current thicknesses spans 110–3000 m (Hendrix et al., 1992; Chen et al., 2004; Yixin and Pengwan, 2009). This dramatic thickness range testifies to the importance of salt flow, which thinned and thickened the unit laterally. Where the salt units thicken toward the south, deformation is concentrated in the suprasalt sequence. From west to east, salt décollements in Kuqa fold-thrust belt have developed into salt nappes exposed at the surface, triangle zones and pop-up structures (Chen et al., 2004; Wang et al., 2011; Li et al., 2012). The suprasalt sequence (Oligocene–Quaternary) reaches a thickness of ~7 km (Tang et al., 2004; Li et al., 2014). The salt-dominated Kumugeliemu Group in western Kuqa fold-thrust belt (Fig. 1) outcrops at line-sourced and point-sourced salt structures. These surface salt structures display structural and stratigraphic records of active vertical motion, exhumation and surface flow (Li et al., 2014).

Point-sourced salt structures, like Awate namakier, Bozidun namakier and an unspecified structure referred to hereafter as Daxiagu namakier, are fed from a salt source via pipe-like feeders (i.e., stems) (e.g., Jackson and Talbot, 1986). Awate namakier occurs at the western extent of the Quilitage anticline system, divided by a south-flowing river. The eastern portion of Awate namakier is approximately 2.5 km long and 1.5 km wide. The western portion may have the same salt source (Li et al., 2014). Salt mining at

the southern edge of Awate exposes freshly cut outcrop surfaces and reveals a mud-rich, 1–3 m thick carapace above the namakier. Bozidun namakier is located ~17 km north of Awate with a length of ~2.2 km and 1.4 km width. Lastly, Daxiagu namakier is the westernmost surface salt structure in Kuqa, located ~12 km west-northwest of Awate. Daxiagu is ~4.5 km long and 3.4 km wide and we interpret it to be a point-sourced based on its circumscribed surface geometry.

Line-sourced salt structures such as Quele namakier and Tuzimazha salt wall have relatively thin, elongated salt feeders (e.g., Jackson and Talbot, 1986). The Quele salt thrust propagates southward and the salt décollement is exhumed where the thrust fault intersects the surface, forming the Quele namakier. Quele namakier is exposed across ~32 km E–W with a vertical thickness generally ranging from ~50–200 m. The namakier thins and locally pinches out toward the west and the salt thrust extends to a north-trending, salt-lubricated strike-slip fault that appears to transfer slip to another E–W trending thrust fault further north (Zhong and Xia, 1998; Li et al., 2014). Quele namakier broadens at its eastern extent and covers an area ~5 km wide, called the Chaerhan namakier, which also features an isolated salt dome (Li et al., 2014). Large, siliciclastic rock bodies, of varying sizes reaching up to 2.5 km length, occur across Quele namakier. These rock bodies may be considered rafts if that have been dislodged from surrounding sedimentary units and incorporated into the namakier as it flows. These sedimentary bodies may also be the more brittle, siliciclastic rocks that make up the Kumugeliemu Group. Toward

the north in the hinterland of Kuqa, the subvertical Tuzimazha salt wall trends east–southeast and maintains an ~ 50 m thickness along its ~ 10 km long surface exposure.

2.2. Subaerial salt deformation and the impact of weather conditions

Relatively low viscosity and density as well as a strong resistance to compression allows rock salt to flow as a non-Newtonian fluid that can pierce through surrounding sedimentary layers in the Earth's upper crust (e.g., Weijermars et al., 1993). Microstructural analysis shows that salt flow converges and accelerates as it moves from a buried source layer into a diapiric feeder, or stem (Desbois et al., 2010). The principal deformation mechanisms observed at the stem of the diapir are grain-boundary migration (GBM) and sub-grain rotation (SGR) caused by increased differential stress (Desbois et al., 2010). Exhumation of salt initially forms salt domes that later develop into salt fountains as circumferential lateral spreading propagates away from the orifice (e.g., Kehle, 1988). Dominant deformation mechanisms shift from GBM and SGR to pressure-solution accommodated grain-boundary sliding (GBS) from the top to the distal part of the salt fountain (Desbois et al., 2010). This shift can be explained by the influx of meteoric water and the decreased differential stress as salt flow divergences radially away from the orifice (i.e., Jackson, 1985; Desbois et al., 2010). A ground-based geodetic study, with hourly to daily sampling, of the Kuh-e-Namak namakier in southern Iran proposed that the presence of meteoric water causes plastic deformation of the salt while daily temperature variations cause elastic deformation (Talbot and Rogers, 1980). Temporary surface salt flow rate of ~ 500 mm/day was observed at Kuh-e-Namak namakier shortly after a large rain event (~ 330 mm average rainfall from October to February) (Talbot and Rogers, 1980). Furthermore, it was observed that during dry periods the surface salt shrunk, retreating and losing some of lateral extent attained during the wet period (Talbot and Rogers, 1980).

Given the typical low-pressure stress conditions of subaerial salt bodies, the namakier porosity is stimulated by joints formed as a result of diurnal/seasonal thermal expansion and contraction (Merriam et al., 1962; Talbot and Aftabi, 2004; Desbois et al., 2010). Vertical joints in subaerial salt bodies dilate as the salt carapace spreads in response to continual growth of the viscous salt fountain, which permits infiltration of meteoric water (Desbois et al., 2010). The carapace of a namakier is typically composed of granular clastic material left behind after the shallower layers of salt have dissolved (e.g., Walker, 1973). An annual temperature range of -0.5 °C to 37.8 °C was enough to facilitate the plastic deformation observed at Kuh-e-Namak (Talbot and Rogers, 1980). However, surface motion during dry periods not only depends on temperature but also the thermal gradient in the salt, which is dependent on the wetness of the salt (Talbot and Rogers, 1980). The semi-arid climate of the Kuqa fold-thrust belt allows the preservation of subaerial salt exposures. Here, annual rainfall averages ~ 74 mm (April–October) and average temperatures can range from -13.3 °C to 31.2 °C.

2.3. Models, predictions, and tests

The rapid kinematic response of surface salt structures to temporary stimuli requires subaerial salt evolution analysis to consider short-term (days to years) deformation kinematics. The rates of salt supply, salt dissolution, sediment accumulation of the overburden, erosion and regional tectonic strain influence the long-term evolution of a namakier (i.e., Koyi, 1998; McGuinness and Hossack, 1993). Crustal shortening may impede diapirism if lateral compression results in an obstruction of the salt feeder (Koyi, 1998). In

other circumstances the compression of a diapir feeder may physically separate the diapir from the source layer. This can produce a temporary pulse of increased salt extrusion rates that would mark the onset of the final phases of namakier evolution (Koyi, 1998).

Extreme daily temperature variations in semi-arid climates, like Kuqa fold-thrust belt, lead to oscillating inflation and deflation of a subaerial salt body on a sub-hourly to daily scale (Talbot and Rogers, 1980). We would expect the entire surface of the namakiers to uplift during daylight hours, when surface temperatures can be very high, under the influence of thermal expansion (Merriam et al., 1962). Similarly, we expect subsidence across the namakier surfaces, as a result of thermal contraction, when temperatures drop well below freezing. Hourly sampling, at minimum, of temperature and surface motion would be necessary to detect the rate and degree of daily oscillations across the namakier surfaces at Kuqa fold-thrust belt. Similar inflation and deflation cycles in response to seasonal variations may also be detectable. However all these variations due to the thermal expansion or contraction of the salt body are likely small because the coefficient of the very low thermal expansion of NaCl, in the range of $5 \cdot 10^{-6}$ °C⁻¹ (White, 1965). For example, in the idealized case of a homogeneous variation of 40 °C on a 1 m thick salt layer, these thermal effects would result in a vertical displacement of the order of 200 μ m.

The short-term deformation patterns of namakiers must consider moisture at the surface. When sufficient quantities of meteoric water make contact with/infiltrate namakiers, pressure-solution and grain boundary sliding allow accelerated salt flow. We expect namakiers at Kuqa fold-thrust belt to flow faster within days after storm and rain events. As salt flow accelerates the leading edge of the surface salt bodies should extend further laterally. As a namakier spreads laterally, the surface should appear to subside. This can be visualized for a static namakier by considering how a drop of molasses would behave on a tabletop. As the drop spreads slowly in every direction, the surface will flatten, bringing the top of the molasses closer to the table.

Two models suggest conflicting roles of the carapace in surface salt kinematics during dry periods. One scenario is the dry-inflation model that suggests the carapace that develops on a surface salt body inhibits lateral spreading and facilitates swelling at the dome (above the orifice) as the salt extrudes from the feeder (Talbot and Pohjola, 2009). If this model holds for Kuqa fold-thrust belt then we should see a relative surface uplift above the orifice during dry periods. Alternatively, dry-deflation model suggests that the carapace hinders uplift of the central dome and instead promotes lateral spreading (Aftabi et al., 2010). With a constant salt supply rate, this model suggests a continual surface subsidence of the namakier as it spreads laterally. To test these models we must record time-lapse surface motions of the Kuqa fold-thrust belt namakiers during wet and dry periods as well as document the occurrences of rain events.

The resistance supplied by a load overlying the orifice of a namakier is another factor that can potentially impact subaerial salt. Emergent, surface breaching, diapirs rise faster than pre-emergent diapirs because of the reduced confinement and load when the overburden is removed (e.g., Weinberg, 1993). Strain rates from microstructural analysis for pre-emergent diapirs range from 10^{-15} to 10^{-13} s⁻¹ while higher strain rates from 10^{-11} to 10^{-9} s⁻¹ have been observed for emergent diapirs (Talbot and Jackson, 1987). This aligns with flow velocity estimates that show pre-emergent diapirs in Germany rise ~ 0.3 mm/yr while emergent diapirs in Iran can exceed 10 mm/yr (e.g., Trusheim, 1960; Talbot and Aftabi, 2004). Strain and velocity rates of pre-emergent and emergent diapirs reasonably suggest that the rate of salt extrusion can increase if enough material above the orifice of a namakier is removed. The salt above the orifice is a load, and this

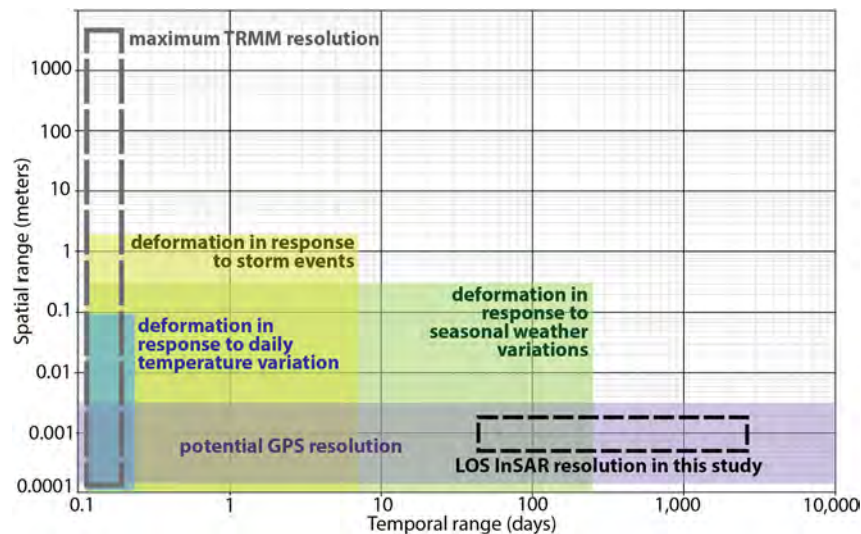


Fig. 3. Logarithmic plot with spatial range in meters over temporal range in days. The yellow, green and blue regions represent the range of temporal and spatial scales that deformation in response to respective variables could be observed. The purple highlights possible GPS sampling resolution. The dashed black rectangle represents the range of spatial and temporal sample of our Envisat dataset. Satellites like the Sentinel 1A and 1B have potential to reach temporal resolution of up to 5 days. The dashed gray rectangle represents the maximum Tropical Rainfall Measuring Mission (TRMM) resolution used in this study. (For interpretation of the references to color in this figure legend, the reader is referred to the web version of this article.)

load is reduced by salt spreading away from the orifice at the surface.

Removal of material above the orifice can occur via erosion and salt dissolution. During periodic large storm events, the shallow, relatively uncompact layers of the namakier carapace can erode considerably (Wenkert, 1979). Furthermore, significant salt dissolution can occur during storm events if the carapace thickness allows sufficient meteoric water to infiltrate the namakier. In the event that the removal of material above the orifice is large enough, we expect acceleration of salt extrusion resulting in an overall rise of the namakier surface. Conversely, if the load above the namakier orifice controls the salt extrusion rate, a thickening carapace would cause a deceleration of salt extrusion that would also lead to a deceleration of lateral spreading.

3. Methods

To better understand the complex set of processes that govern deformation in salt bodies, we examine several different bodies using a diverse set of data, including space-based constraints on ground deformation and weather information from both ground stations and remote sensing. Surface salt deformation is accessed using a remote sensing technique called interferometry of synthetic aperture. To perform the InSAR analysis we utilize Envisat ASAR (Advanced Synthetic Aperture Radar) imagery acquired between June 2003 and October 2010. To access the relationship between subaerial salt motions and weather conditions we use Tropical Rainfall Measuring Mission (TRMM) data and local weather station data during the same period of Envisat acquisitions. The temporal resolution of the Envisat imagery available must be less than the temporal range of surface salt motion to detect the salts' kinematic responses to weather variations (Fig. 3). Because of this it is unlikely that our Envisat dataset could resolve the impact of individual storm events as our best temporal resolution is 36 days. However, it is possible to detect the impact of seasonal weather variations. The combination of these disparate datasets, which have very different spatial and temporal resolutions and degrees of uncertainty, presents some challenges, but also allows a more complete analysis of the setting.

3.1. Weather estimates

The TRMM satellite has utilized microwave and radar instruments since late 1997 with a spatial coverage between latitude 50°S to 50° (Huffman, 2011). The Daily TRMM Rainfall Estimate (3B42 v7) used for our analysis is a product derived from rain gauge and multiple TRMM satellite measurements. First, independent precipitation estimates from various microwave instruments are calibrated to TRMM Combined Instrument (TCI) precipitation estimates (Huffman, 2011). The 3-hourly multi-satellite measurements are combined with the accumulated monthly Global Precipitation Climatology Centre (GPCC) rain gauge analysis using inverse-error-variance weighting to form a monthly best-estimate precipitation rate (Huffman, 2011). Lastly, the 3-hourly estimates are scaled for the month then summed to the monthly value for each individual grid box (Huffman, 2011). The final data set has precipitation estimates with a 3-hourly temporal resolution and a $0.25^\circ \times 0.25^\circ$ spatial resolution (Huffman, 2011). This temporal resolution is sufficient to observe storms that can occur in the span of a few hours across the surface salt structures in Kuqa fold-thrust belt.

Another dataset we have used includes daily humidity, temperature, and rainfall measurements from a meteorological weather station in Kuqa, Xinjiang Province, China (Tutiempo Network, 2015). We utilize this station, despite its location over 150 km away, because it is the closest ground truth. When we compare the rainfall estimates from the weather station and the TRMM dataset we look at the cumulative measurements for the time periods between each Envisat image acquisition. Similarly, we compare the average surface temperature and humidity during each time period between image acquisitions.

3.2. Interferometry of synthetic aperture radar (InSAR)

We constructed an InSAR time series to constrain the surface displacements of active extruded salt structures in western Kuqa fold-thrust belt as well as several surface displacements associated with hydrocarbon withdrawal and subsurface fluid injection. InSAR is a remote sensing technique that uses radar imagery to provide spatially dense measurements of surface displacements

in the satellite line of sight (LOS) with millimeter to centimeter accuracy (e.g., Zebker et al., 1994; Massonnet and Feigl, 1998; Bürgmann et al., 2000). Multiple SAR images are used to generate sets of interferograms to form a time series after a joint inversion (e.g., Bernardino et al., 2002). InSAR time series analysis helps reduce the impact of several noise sources (decorrelation, orbital and DEM errors, atmospheric delays, phase unwrapping errors) on displacement rates estimates during the time period spanned by the full dataset (e.g., Grandin et al., 2012) with an accuracy for surface displacement velocity at the mm/yr scale. The time series analysis also allows identification of time variable deformation including seasonal signals and response to earthquakes or anthropogenic activity.

We use 40 ESA ASAR C-band radar images acquired by the Envisat satellite between June 2003 and October 2010 from Track 291 (along descending orbits). A small-baseline approach (e.g., Bernardino et al., 2002) was used to process interferograms and invert for average displacement rates and evolution through time with the New Small Baseline Algorithm Subset (NSBAS) chain, as described in detail by Doin et al. (2012) and Jolivet et al. (2013). 85 individual interferograms were generated using a modified version of the Caltech/JPL Repeat Orbit Interferometry Package (ROI_PAC, Rosen et al., 2004) and the STRM 90-global DEM. Interferograms were corrected from DEM errors (Ducret et al., 2014) and stratified tropospheric delays (based on the ERA-Interim global atmospheric model, Doin et al., 2009; Jolivet et al., 2011), multi-looked by a factor of 4 in the range direction and 20 in the azimuth direction, flattened and filtered before unwrapping. Individual interferogram coherence was used to determine the optimal unwrapping path for each interferograms. The phase unwrapping was achieved iteratively, beginning in areas of high coherence then incrementally reducing the coherence threshold for each iteration (Grandin et al., 2012). The InSAR inversion process does not allow for a direct measurement of the error margin of the LOS displacement measurements, however we estimate the noise level is on the order of ~ 1 mm/yr. Radar amplitude images were used to interpret the namakiers' boundaries, outlined on the velocity maps.

We present average velocity (mm to cm/yr) and displacement maps with a spatial resolution of 80×80 m. The velocity and displacement maps are displayed in line of sight (LOS) with positive (red) and negative (blue) values corresponding to movement toward and away from the sensor that we furthermore interpret as uplift and subsidence, respectively, due to the dominant sensitivity of InSAR to vertical motion. Differential incremental displacement maps and time series are used to track the temporal phase evolution. To isolate relative displacements, we generate these differential maps and time series computing the difference between time series from points within deforming areas and time series from local reference points. This helps minimizing the effect of spatially coherent noise. The remaining, relative, correlated temporal fluctuations observed and comparisons to weather conditions are discussed in the following section.

The present study uses three datasets that were processed to obtain a time-series that cover the period June 2003 to October 2010 where InSAR data provide estimates of surface displacement at a pixel size of ~ 30 m and time resolution of 36 to 210 days, with an average of 75 days. From the nearest weather station, average temperatures and precipitations are obtained. Finally, the TRMM data provide the same time-lapse series as the weather station, at a pixel size resolution of 4 km and for the same periods at the InSAR data. These three data sets are then processed to 1) analyze the surface deformation of salt bodies, 2) correlate these deformations with weather conditions.

4. Results

4.1. Kinematic observations

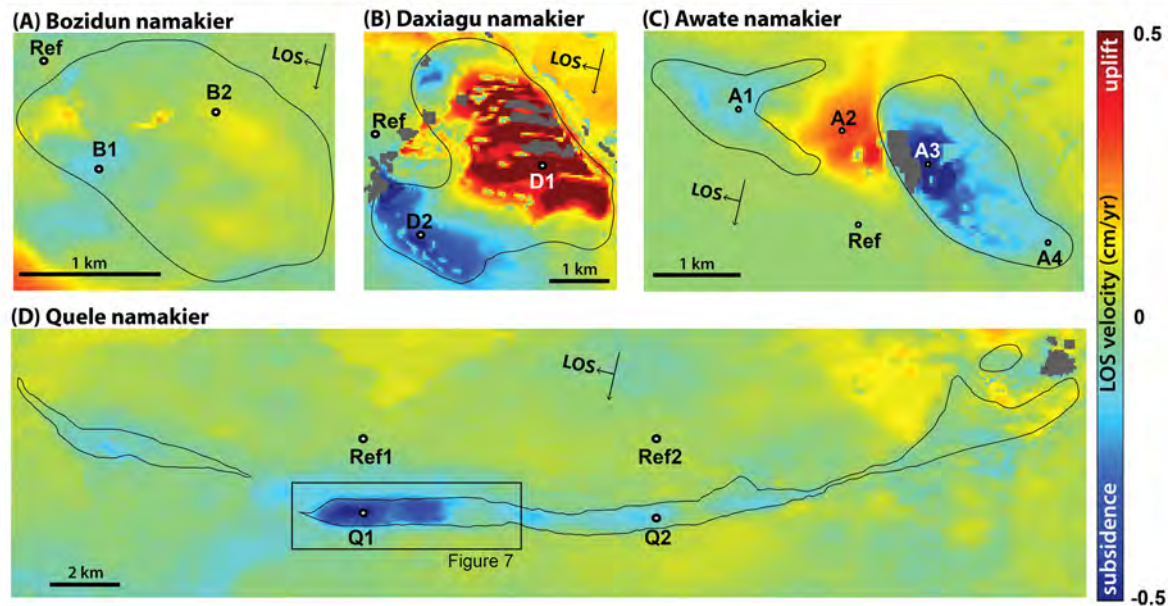
The overall distribution of LOS velocity at Bozidun namakier is relatively uniform. From the average velocity map, minor subsidence is observed on the western margin and localized uplift near the north and east (Fig. 4A). The velocity distribution across Bozidun namakier is nearly indistinguishable from its immediate surroundings supporting field observations that suggest Bozidun namakier is not actively extruding material to the surface, as shown in the time series of the Fig. 4.

The distribution of positive and negative LOS velocities at Daxiagu is asymmetrical and ranges from -4.5 to 5 mm/yr (Fig. 4B). An area of uplift is observed on the northeastern side of the structure, oriented toward the northwest. Areas of overall subsidence occur predominately on the southwestern side of the structure as well as the northwestern. The incremental displacements maps highlight deformation patterns that do not reflect the long-term deformation patterns measured by the average displacement velocity maps (Fig. 5). Each incremental displacement map of Daxiagu displays relatively uniform deformation across the namakier with fluctuations between surface uplift and subsidence at different time intervals. Time series analysis of east and west Daxiagu namakier inversely mirror each other; the east is uplifting at approximately the same rate (~ 4.5 mm/yr) as the west is subsiding. The ribbed pattern that appears in both the average velocity map and the incremental displacements maps do not correlate to topographical variations but instead may reflect noisiness in the data likely due to the namakiers' rugged surface.

Displacement velocities at Awate namakier are distributed asymmetrically (Fig. 4C). Awate namakier is divided in two by a major river with stronger subsidence observed on the eastern segment, slight subsidence on the west, and uplift at the river channel in between. On the eastern Awate namakier the displacement velocities decrease radially away from the center and the maximum rate of displacement approaches -5 mm/yr. Incremental displacement maps show that the east Awate namakier has experienced periods of uplift despite overall subsidence suggesting it is an active structure. The areas of displacement at east Awate namakier have consistent shapes in the incremental displacement maps for periods of a year to three, but gradually shift from a central block to a more variegated area. These areas all subside and uplift more dramatically than the surroundings. Minor subsidence and unvarying incremental displacements are observed at west Awate namakier. Localized uplift at the river channel approaches 4 mm/yr. The zone of uplift is broader than the river channel, extending farther to the west. Incremental displacement maps show uplift at the riverbed, dividing Awate namakier, initiated toward the western riverbank then propagated toward the center. The time series analysis at the river channel is notably less noisy and fluctuating than the time series from areas across the namakier, especially for east Awate namakier (Fig. 4). This observation indicates that uplift at the river channel is relatively regular and constant while displacement of the namakier is relatively irregular.

The distribution of average displacement velocities across Quele namakier is predominately uniform (Fig. 4D). Relative subsidence is measured along the exhumed thrust sheet but strong, localized subsidence is observed at the central segment of Quele namakier where the average displacement velocity approaches ~ 4 mm/yr. Velocities measured at Chaerhan namakier and the isolated salt dome at the eastern extent of Quele are within the noise level of background velocity measurements. A few periods of minor uplift are observed in the incremental displacement maps at the central segment despite the overall subsidence suggesting an actively

Average surface displacement rate maps



Time series analysis of surface salt structures

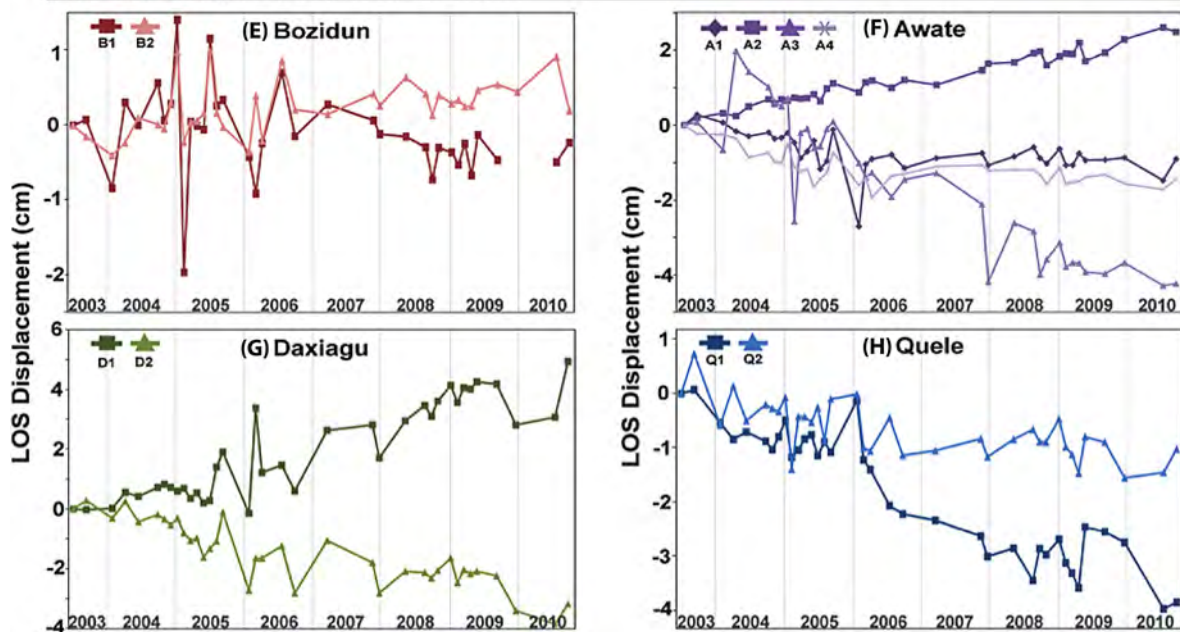


Fig. 4. (Top) Average surface velocity maps for Bozidun namakier (A), Daxiagu namakier (B), Awate namakier (C), and Quele namakier (D) displayed in satellite line of sight (LOS) and saturated to the color scale 0.5 to -0.5 cm/yr. Surface movement toward (uplift) and away (subsidence) from the satellite is represented by warm and cool colors, respectively. (Bottom) Differential time series analysis of select points on Bozidun, Daxiagu, Awate, and Quele namakiers (locations are highlighted by black circles on the velocity maps above) is displayed in LOS displacement (cm) across time (from June 2003 to October 2010). The displacement measurements are relative to local references represented by the label “Ref”. (For interpretation of the references to color in this figure legend, the reader is referred to the web version of this article.)

extruding structure (Fig. 4). Time series analysis shows the displacement trends of two areas in the central segment partially mirror each other, from 2003 to 2006. After 2006, higher rates of subsidence are concentrated toward the east suggesting heterogeneities along the salt thrust.

4.2. Correlation between kinematics and weather conditions

To test the relationship between weather conditions and surface displacements of namakiers in Kuqa fold-thrust belt we compare

the incremental displacements between each image acquisition to the average humidity, average temperature, and cumulative rainfall during the respective time intervals (Fig. 6). There is no clear correlation between average humidity estimates and surface displacements for any of the studied namakiers. Similarly, no correlation is observed between displacements and average temperature for Quele namakier. Furthermore, correlation coefficients between surface displacement measurements on across the 4 namakiers studied and average temperature and humidity estimates yield a maximum correlation of 0.2. However, at Awate, Bozidun and Dax-

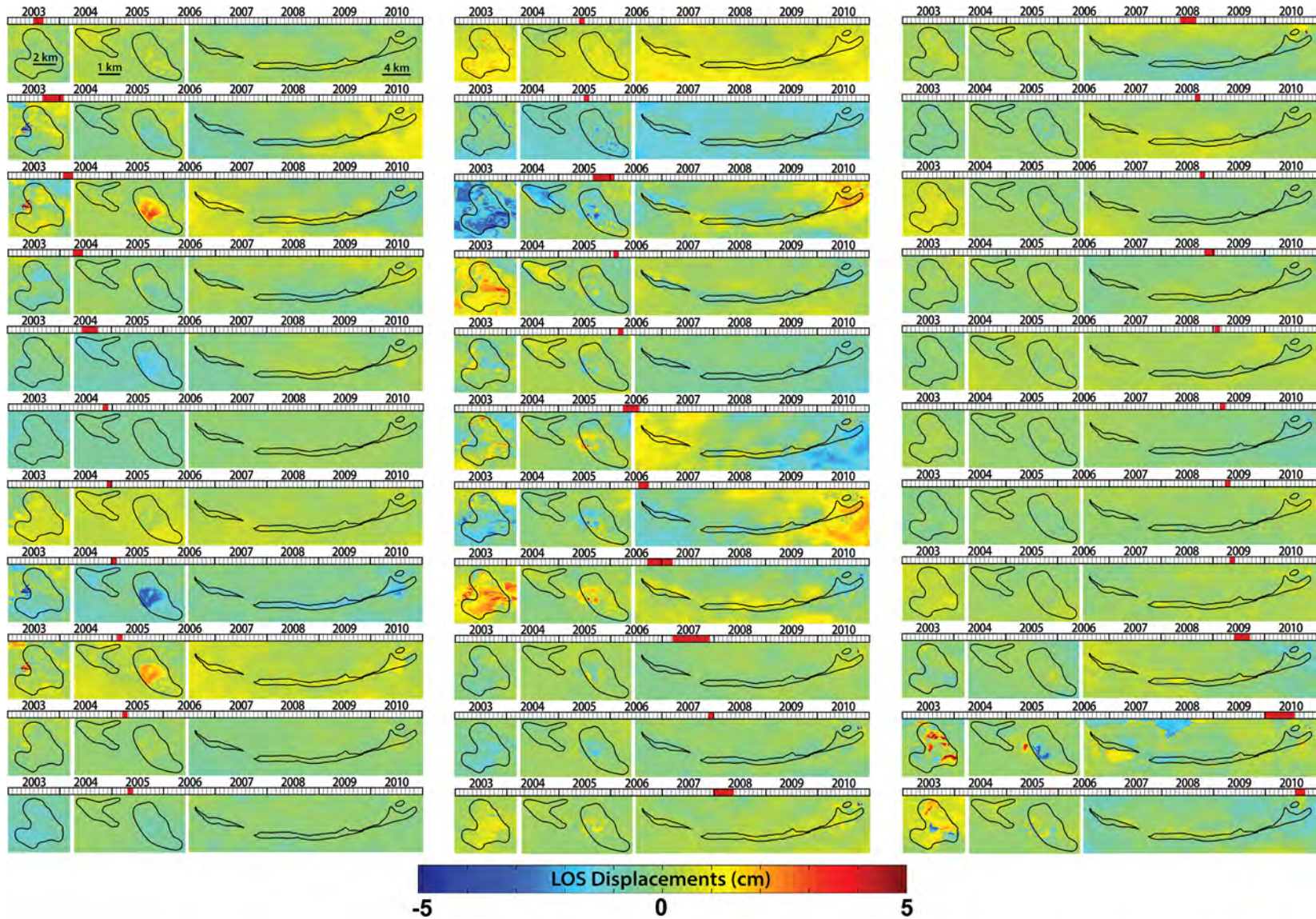


Fig. 5. Line-of-sight (LOS) differential incremental displacement maps of Daxiagu (1A–33A), Awate (1B–33B), and Quele namakers (1C–33C), saturated to the color scale 5 to -5 cm. Displacement values of the local reference points (labeled in Fig. 4) were removed from each incremental displacement map (*Ref1* was used for Quele namaker) to reduce spatially coherent noise and highlight relative motion. Each incremental map spans the time between 2 successive acquisitions, the temporal coverage is represented by the shaded red area on each timeline. (For interpretation of the references to color in this figure legend, the reader is referred to the web version of this article.)

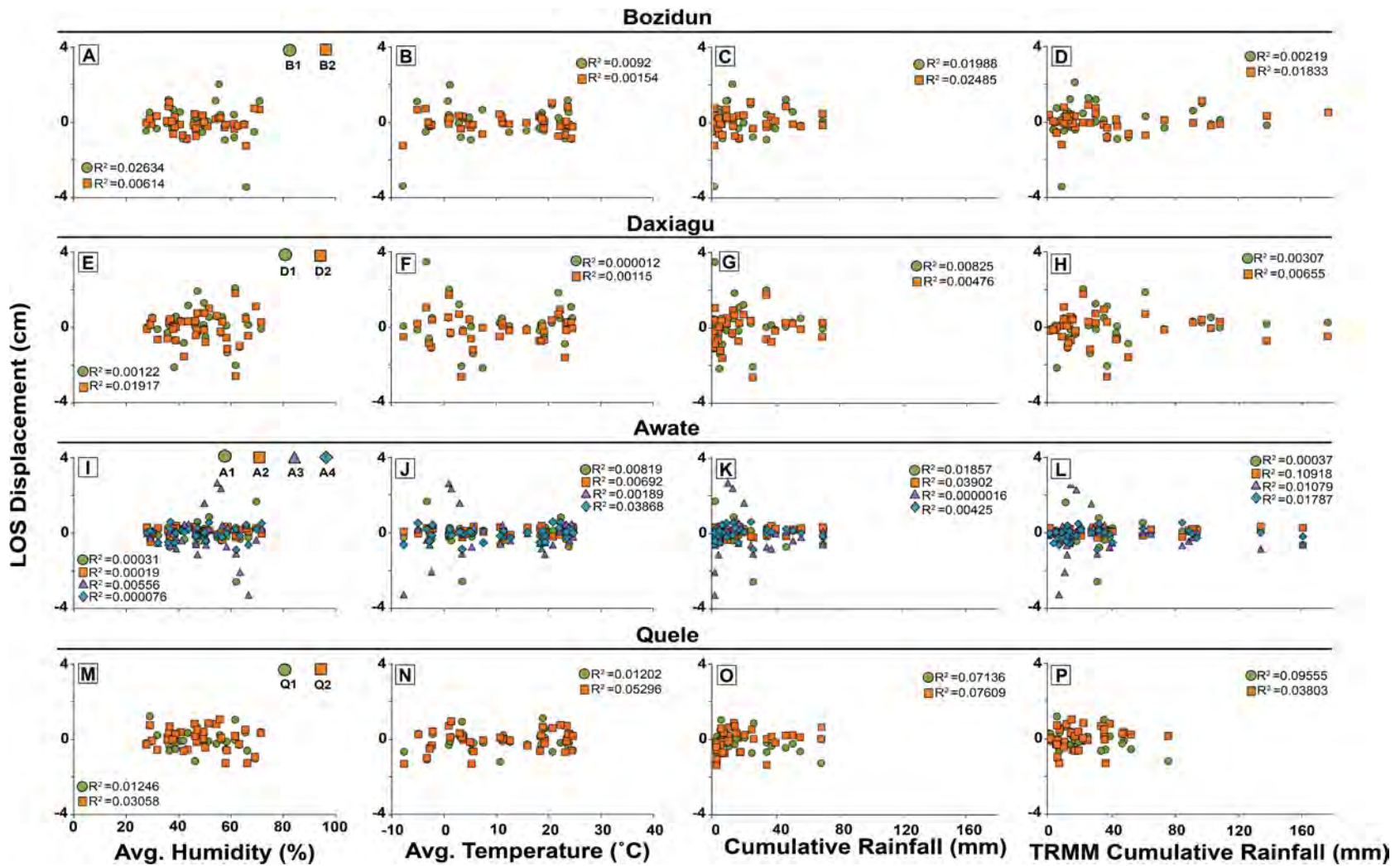


Fig. 6. Comparison between surface displacements at Kuqa fold-thrust belt and weather conditions. We evaluate the dependence of incremental LOS displacement rates (cm) from each structure (Bozidun, Daxiagu, Awate, and Quele namakers) to daily humidity (left), temperature (center left), and rainfall/snowmelt measurements (center right) at a meteorological weather station in Kuqa (Xinjiang Province, China) from Tutiempo Network and daily cumulative rainfall estimates from the Tropical Rainfall Measuring Mission (right).

iagu namakiers we see temperature extremes are associated with more surface salt motion than intermediate temperatures. When we compare the displacements observed at the namakiers to the cumulative rainfall values estimated by TRMM as well as the distantly located weather station, we find a positive correlation. There is an increased occurrence of surface salt displacements during time intervals that experienced lower rainfall estimates suggesting that with less rainfall there is more surface motion. The correlation observed is not simply an artifact of having more data during periods of lower rainfall events because there are equal amounts of temporal coverage during the rainy (April–October) and dry seasons (October–April).

Another way to test the correlation between observed surface displacements and rainfall is to look at how the displacement residuals correlate to rainfall estimates. The residuals of a dataset are the observed values minus the predicted (or average) values. Residuals highlight the data points' deviation from the linear average, which are used to test the correlation between rainfall and surface salt displacement response. When we calculate the correlation coefficient between the residual time series displacements, showing the deviation of each displacement data point from the average, at the namakiers of interest and TRMM rainfall we find no correlation greater than 0.1. The low correlation coefficient is likely due to the occurrence of both positive and negative motion with hot and cold temperatures.

5. Discussion

InSAR analysis uncovers a variety of ground motions across the subaerial salt structures of the Kuqa fold-thrust belt. While the majority of the namakiers studied show surface motion, InSAR estimates of surface motion at Bozidun and Chaerhan namakiers are relatively indistinct from the surrounding area. The lack of observable deformation at the Tuzimazha salt wall could mean that (1) the salt wall has recently become inactive, (2) it is deforming at rates below our detection threshold (<1 mm/yr), or (3) the activity is confined to a small area that is more challenging to resolve. We favor the third interpretation because the thickness of the Tuzimazha salt wall (~ 50 m) cannot be adequately resolved by the 80×80 m spatial resolution of our InSAR dataset (Fig. S4). The namakiers exhibit asymmetrical spatial displacement patterns with fluctuating deformation rates over varying temporal scales (weeks to months). Average velocity estimates in addition to the incremental displacement steps allow us to explore the seasonality of subaerial salt deformation and its link to weather conditions.

5.1. Daxiagu namakier

The asymmetric displacement patterns observed at Daxiagu namakier (Fig. 7A) do not conform to the expected radial flow pattern of a salt fountain. The irregular shape and flow kinematics is likely controlled by the surrounding topography and sub-salt morphology beyond the feeder, beneath the namakier. A river east of Daxiagu has eroded steep channel walls, and likely rapidly dissolves salt that flows toward the east.

Because surface uplift is expected directly above the feeder (orifice) of a point-source namakier, we interpret the area of overall uplift, on the eastern side of the namakier, to indicate the location of the salt feeder. Long-term average uplift also suggests that the rate of salt extrusion into the namakier exceeds the rate of salt dissolution/erosion. The similarity in magnitude of surface displacement on the east and west may indicate the two sides of the namakier are not mutually exclusive (Fig. 4). Diminutive subsidence at the northwestern margin could also indicate partial flow toward the northwest from the namakiers' feeder. Eastward flow

is expected, where a river passes, but the material that flows toward the river is likely dissolved relatively rapidly. The subsidence is interpreted to reflect an approximate volume balance as the namakier spreads farther out. This interpretation suggests that the dominant direction of flow is toward the west and that lateral spreading is faster than the rate of supply. The southwestern lobe of Daxiagu is subsiding on average, but does not appear in the time-lapse data in any one time-step. However, we find no statistical correlation to suggest weather conditions control the surface motion patterns measured. Furthermore, this observation is not likely to be climatically driven because we do not see it in incremental displacement maps. The north-south tectonic shortening (~ 4 – 7 mm/yr) accommodated across the Kuqa fold-thrust belt is likely to have a greater influence on the exhumation rates and subsequent surface displacement patterns (e.g., Allen et al., 1991; Zhong and Xia, 1998; Yang et al., 2010; Zubovich et al., 2010). However, to positively discriminate the precise influence of regional shortening on subaerial salt motion, spatially dense GPS observations are necessary across the area.

5.2. Awate namakier

Subsidence is concentrated at the center of the eastern Awate namakier (Fig. 7B). The broad, long-term deformation pattern of centralized subsidence is indicative of a mature namakier that is experiencing a dissolution/erosion rate which exceeds the rate at which salt is fed into the structure. Distinct anthropogenic forcing may play a role: salt mining operations spray water along the southwestern margin of the eastern Awate namakier branch, which may influence the observed long-term subsidence by locally increasing salt dissolution.

Incremental displacement maps do not entirely correspond with observations from the average displacement velocity map, thereby revealing different deformation patterns at different temporal scales. Unlike the long-term displacement pattern, four intervals of incremental surface uplift at eastern Awate namakier occur between January and March (colder/drier months) confirming that new material (salt) is being fed into the namakier. We observe uplift when our temperature-kinematic salt models predict Awate would experience overall surface subsidence during colder periods in response to thermal contraction. Calculated correlation coefficients between incremental displacements and temperature variations show no statistical correlation. Temperature variations do not appear to control periods of wide spread uplift and subsidence. The intervals of uplift do, however, support the dry-inflation model. The dry-inflation kinematic salt model predicts a namakier will inflate during dry periods because the carapace inhibits lateral spreading. At Awate namakier, we observe uplift above a central location (dome) during periods of low rainfall implying that the carapace restricts lateral spreading and prefers dome inflation during dry periods. Furthermore, periods of increased rainfall do not correspond to increased surface salt uplift.

The average, long-term (~ 7.3 yr) uplift signal measured at the river channel between the east and west segments is not notably observed in the incremental displacement maps. If river deposition were responsible for the rise of the river channel surface between the Awate namakier branches, the area of uplift would not be as localized as observed. Instead, the rise would continue as the river does, toward the south. It is more likely that the concentrated uplift observed at the river channel is due the rise of salt from the source layer through the stem of the diapir that feeds Awate namakier. If the river cuts off the salt feeder that sources Awate, the observed uplift could be the result of accumulating strain in the overburden of a partially buried, active salt feeder. However, the estimated long-term rate of uplift here is not likely to persist for time scales of >100 yr because that would significantly perturb

InSAR surface displacement rates and kinematic interpretations

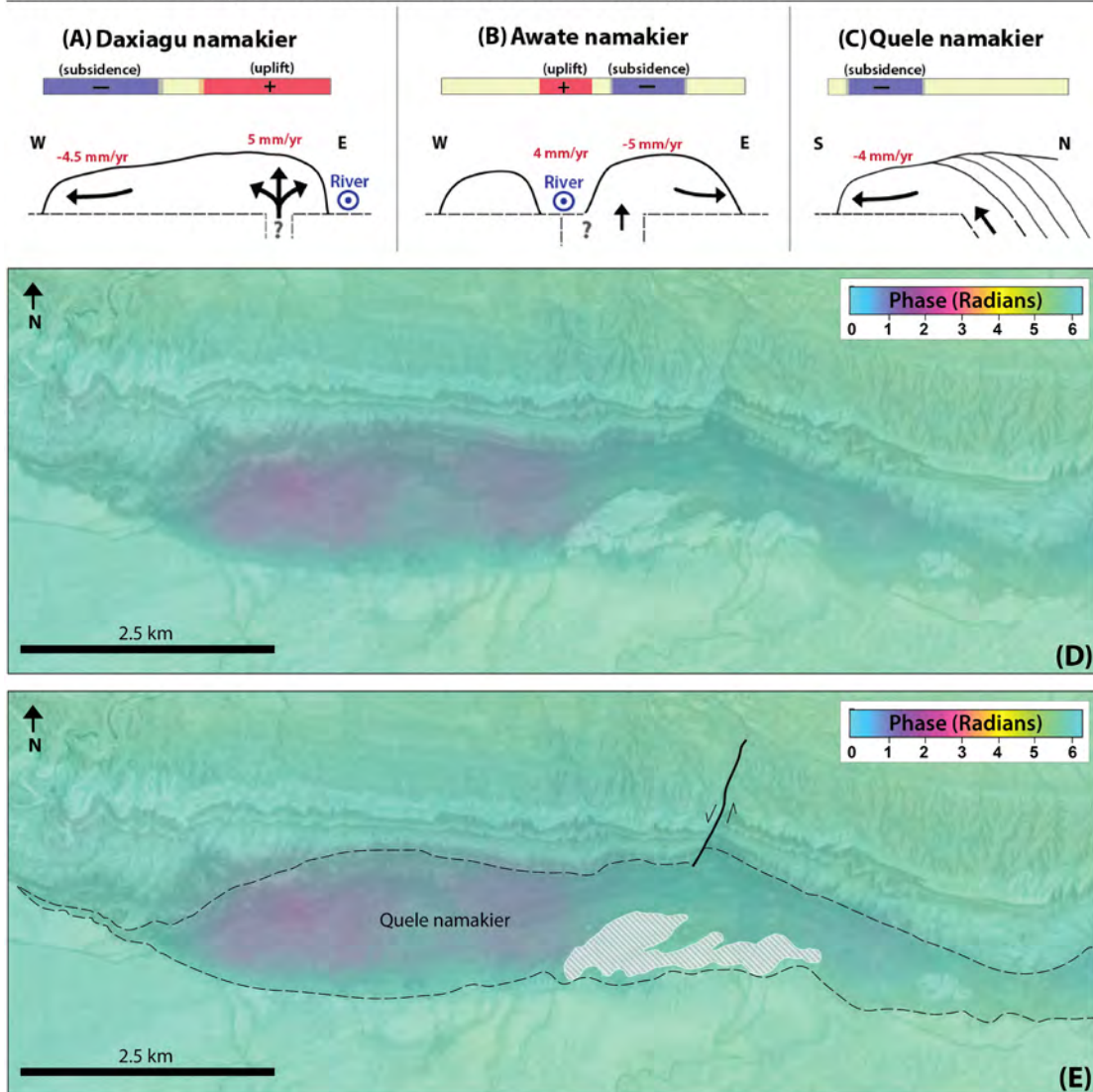


Fig. 7. (Top) Schematic cross-section and overview of displacement patterns across Daxiagu, Awate and Quele namakiers and kinematic interpretations. Daxiagu is interpreted to have an inflating dome that actively extrudes from salt feeder on the eastern side. Similarly, Awate is interpreted to flow predominantly toward the east to southeast. Awate is interpreted to have a salt feeder on the eastern segment that may be partially buried by the adjacent river channel causing the localized uplift. Unlike Awate and Bozidun namakiers, Quele namakier does not have a central dome because it is an exhumed salt thrust décollement. We interpret the dominant flow direction of Quele namakier to be toward the south. (Bottom) The average displacement map (displayed in radians) overlaid on top of Google Earth. The concentrated area subsidence at Quele corresponds precisely to a large raft immediately to the east of the area of deformation. The local left-lateral tear fault may also have created a structure barrier between this part and the rest of the namakier. (For interpretation of the colors in this figure, the reader is referred to the web version of this article.)

the long-term equilibrium topography by developing a hill in the very place there is a river. It is possible to perturb the equilibrium topography if the diapir is new or suddenly changing character, but it is not new because the namakier is well established. Thus, we interpret the equilibrium to be controlled by the regular frequency of large flooding events allowing this area to neither rise nor fall with respect to regional baseline for longer periods than ~ 7 yr. Alternatively, the surface of the river channel in between the Awate namakier can be controlled by a natural equilibrium between the diapir extrusion rate and river erosion. A study of climatic conditions from 1951 to 2009 in Xinjiang, China reveals that the average precipitation has increased by 15 mm since 1990 (Kong and Pang, 2012). To our knowledge, a detailed study of this particular river does not exist, however, work done on the proximal Tailan River, west of Awate, found that glacial melt-water accounts for 60% of its $7.5 \times 10^8 \text{ m}^3$ annual river discharge (Zhao et al., 2015). The combination of increased rainfall and possible glacial melt-water,

due to the 1°C raise in average annual temperature, would facilitate flash-floods every 10 to 100 yr that removes a lot of material through erosion, maintaining a topographic equilibrium (Kong and Pang, 2012).

5.3. Quele namakier

Quele namakier (Fig. 7C) is the exhumed portion of a significant salt thrust and its surface kinematic patterns vary from typical salt fountains. Because it is a line-source structure, we do not expect to see radial flow comparable to a point-sourced structure. Unlike a salt fountain, if the exhumation rate of Quele namakier increases the surface is not likely to uplift significantly because it is confined by its overburden, the hanging wall of the Quele salt thrust. Instead we would see increased subsidence due to amplified southward spreading. Decreased exhumation would result in stagnant to minimal lateral spreading. The overall subsidence

observed across Quele namakier is within the range of the data resolution. However, one area of the structure has experienced a higher rate of subsidence. Weather conditions are unlikely to be responsible because we see no statistical relationship between surface motion and weather variations (temperature and moisture). Furthermore, it is unlikely that weather conditions would exclusively and consistently affect only one spot along a relatively smooth hill-front. Alternatively, the isolated subsidence at Quele namakier may be structurally controlled. The subsidence could be the result of a pinched salt source because analog models by Cotton and Koyi (2000) show that an overriding hanging wall can pinch a salt décollement during shortening. A possible indicator of a pinched salt décollement includes the left-lateral tear fault that occurs in the hanging wall, coincident with the area of concentrated subsidence (Fig. 7E). The tear fault could have resulted from lateral variations along the salt décollement, such as thickness, which could indicate a pinched salt source for Quele namakier. Alternatively, the tear fault may be the result of differential shortening of the thrust sheet. A large siliciclastic rock body, which appears to be a raft, is located along Quele namakier and south of the tear fault (Fig. 7E). If this siliciclastic rock body acted as a structural barrier, limiting southward propagation of the exposed Quele salt décollement (namakier), then it may have caused sufficient differential shortening rates to generate a tear fault. This alternative suggests that the localized, increased subsidence at Quele is the result of differential shortening across one portion of the Quele thrust.

5.4. Limitations

Across Kuqa fold-thrust belt, we discovered that subaerial salt motion is decoupled from weather conditions. The sparse temporal sampling of this Envisat dataset is significantly limited when compared to the daily sampling rate of temperature and rainfall from spaceborne satellites or ground-based weather stations. Additionally, the restricted spatial rainfall resolution of ~4 km estimates from spaceborne satellites may also preclude correlation with meter-scale InSAR sampling resolution. Looking forward, the association of the European Space Agency's Sentinel 1A and 1B could provide improved temporal coverage after several years of observation and better quantify the temporal fluctuations that may reveal the weather dependence we expected.

6. Conclusions

In this study we present quantitative estimates of sub-aerial salt displacement rates of surface salt bodies in Kuqa fold-thrust belt of northwest China. We predicted strong dependence of surface salt motion on weather conditions based on previous surface salt studies but discovered weather conditions do not control surface kinematics here. Although the namakiers occur in the same fold-thrust belt, none of the salt bodies share the same short-term kinematic displacement pattern, which suggests contrasting subsurface geometries between the salt bodies. We measure the dominant vertical displacement and identify asymmetric deformation patterns of uplift and subsidence at Daxiagu and Awate, likely controlled by local tectonics and topography. At Quele namakier we identify an area of concentrated subsidence that is coincident with surrounding structural features that may indicate a pinched salt thrust. Li et al. (2014) detailed the geometries of the Awate, Bozidun, Quele and Daxiagu namakiers. Our study furthers our understanding of the Kuqa fold-thrust belt namakiers by providing a kinematic description of the active subaerial salt motion.

Acknowledgements

We thank two anonymous reviewers for their helpful comments. This work was supported by the Marathon Oil GeoDE Graduate Assistantship at LSU, LA-AMP Bridge to Doctorate Fellowship at LSU, Université Grenoble-Alpes – Institut des Sciences de la Terre (ISTerre), Tarim Oil Company (a subsidiary of the China National Petroleum Corporation), grants from the American Chemical Society Petroleum Research Fund (PRF-53549-ND8), U.S. National Science Foundation (EAR-1322033), and Cornell University Earth and Atmospheric Sciences Department. I would especially like to thank Matthieu Volat and Simon Daout at ISTERre for their technical support. The European Space Agency (ESA) provided the Envisat ASAR imagery used for this study (Dragon project 10686).

Appendix A. Supplementary material

Supplementary material related to this article can be found online at <http://dx.doi.org/10.1016/j.epsl.2016.06.009>.

References

- Aftabi, P., Roustaei, M., Alsop, G.I., Talbot, C.J., 2010. InSAR mapping and modelling of an active Iranian salt extrusion. *J. Geol. Soc.* 167, 155–170.
- Allen, M.B., Windley, B.F., Chi, Z., Zhong-Yan, Z., Guang-Rei, W., 1991. Basin evolution within and adjacent to the Tien Shan Range, NW China. *J. Geol. Soc.* 148 (2), 369–378.
- Baikpour, S., Zulauf, G., Dehghani, M., Bahroudi, A., 2010. InSAR maps and time series observations of surface displacements of rock salt extruded near Garmsar, northern Iran. *J. Geol. Soc.* 167, 171–181.
- Barnhart, W.D., Lohman, R.B., 2012. Regional trends in active diapirism revealed by mountain range-scale InSAR time series. *Geophys. Res. Lett.* 39, 1–5.
- Berardino, P., Fornaro, G., Lanari, R., 2002. A new algorithm for surface deformation monitoring based on small baseline differential SAR interferograms. *IEEE Trans. Geosci. Remote Sens.* 40 (11), 2375–2383.
- Bürgmann, R., Rosen, P.A., Fielding, E.J., 2000. Synthetic aperture radar interferometry to measure Earth's surface topography and its deformation. *Annu. Rev. Earth Planet. Sci.* 28 (1), 169–209.
- Canerot, J., Hudec, M.R., Rockenbauch, K., 2005. Mesozoic diapirism in the Pyrenean orogen: salt tectonics on a transform plate boundary. *AAPG Bull.* 89 (2), 211–229.
- Chen, S., Tang, L., Jin, Z., Jia, C., Pi, X., 2004. Thrust and fold tectonics and the role of evaporites in deformation in the Western Kuqa Foreland of Tarim Basin, Northwest China. *Mar. Pet. Geol.* 21, 1027–1042.
- Cotton, J.T., Koyi, H.A., 2000. Modeling of thrust fronts above ductile and frictional detachments: application to structures in the Salt Range and Potwar Plateau, Pakistan. *Geol. Soc. Am. Bull.* 112 (3), 351–363.
- Desbois, G., Závada, P., Schléder, Z., Urai, J.L., 2010. Deformation and recrystallization mechanisms in actively extruding salt fountain: microstructural evidence for a switch in deformation mechanisms with increased availability of meteoric water and decreased grain size (Qum Kuh, central Iran). *J. Struct. Geol.* 32.
- Doin, M.P., Lasserre, C., Peltzer, G., Cavalié, O., Doubre, C., 2009. Corrections of stratified tropospheric delays in SAR interferometry: validation with global atmospheric models. *J. Appl. Geophys.* 69 (1), 35–50.
- Doin, M.-P., Lodge, F., Guillaso, S., Jolivet, R., Lasserre, C., Ducret, G., Grandin, R., Pathier, E., Pinel, V., 2012. Presentation of the small baseline NSBAS processing chain on a case example: the Etna deformation monitoring from 2003 to 2010 using Envisat data. In: *Proceedings from Fringe 2011 Workshop*. Frascati, Italy, 19–23 September 2011. In: ESA-SP, vol. 697.
- Ducret, G., Doin, M.P., Grandin, R., Lasserre, C., Guillaso, S., 2014. DEM corrections before unwrapping in a small baseline strategy for InSAR time series analysis. *IEEE Geosci. Remote Sens. Lett.* 11 (3), 696–700.
- Grandin, R., Doin, M.P., Bollinger, L., Pinel-Puysségur, B., Ducret, G., Jolivet, R., Sapkota, S.N., 2012. Long-term growth of the Himalaya inferred from interseismic InSAR measurement. *Geology* 40 (12), 1059–1062.
- Hendrix, M.S., Graham, S.A., Carroll, A.R., Sobel, E.R., McKnight, C.L., Schulein, B.J., Wang, Z., 1992. Sedimentary record and climatic implications of recurrent deformation in the Tian Shan: evidence from Mesozoic strata of the north Tarim, south Junggar, and Turpan basins, northwest China. *Geol. Soc. Am. Bull.* 104 (1), 53–79.
- Huffman, G., 2011. Global change master directory – daily TRMM and others rainfall estimate. http://gcmd.gsfc.nasa.gov/KeywordSearch/Metadata.do?Portal=GCMD&MetadataType=0&MetadataView=Full&KeywordPath=&EntryId=GES_DISC_TRMM_3B42_daily_V7. Accessed: 07/2015.
- Jackson, M.P.A., 1985. Natural Strain in Diapiric and Glacial Rocksalt, with Emphasis on Oakwood Dome, East Texas. Bureau of Economic Geology, The University of Texas at Austin, Texas.

- Jackson, M.P.A., Talbot, C.J., 1986. External shapes, strain rates, and dynamics of salt structures. *Geol. Soc. Am. Bull.* 97, 305–323.
- Jolivet, R., Grandin, R., Lasserre, C., Doin, M.-P., Peltzer, G., 2011. Systematic InSAR tropospheric phase delay corrections from global meteorological reanalysis data. *Geophys. Res. Lett.* 38.
- Jolivet, R., Lasserre, C., Doin, M.P., Peltzer, G., Avouac, J.P., Sun, J., Dailu, R., 2013. Spatio-temporal evolution of aseismic slip along the Haiyuan fault, China: implications for fault frictional properties. *Earth Planet. Sci. Lett.* 377, 23–33.
- Kehle, R.O., 1988. The origin of salt structures. In: Schreiber, B.C. (Ed.), *Evaporites and Hydrocarbons*. Columbia University Press, New York, pp. 345–404.
- Kent, P.E., 1979. The emergent Hormuz salt plugs of southern Iran. *J. Pet. Geol.* 2, 117–144.
- Kong, Y., Pang, Z., 2012. Evaluating the sensitivity of glacier rivers to climate change based on hydrograph separation of discharge. *J. Hydrol.* 434, 121–129.
- Koyi, H., 1998. The shaping of salt diapirs. *J. Struct. Geol.* 20 (4), 321–338.
- Li, S., Wang, X., Suppe, J., 2012. Compressional salt tectonics and synkinematic strata of the western Kuqa basin, southern Tian Shan, China. *Basin Res.* 23, 1–23.
- Li, J., Webb, A.A.G., Mao, X., Eckhoff, I., Colón, C., Zhang, K., Wang, H., Li, A., He, D., 2014. Active surface salt structures of the western Kuqa fold-thrust belt, Northwestern China. *Geosphere* 10 (6).
- Massonnet, D., Feigl, K.L., 1998. Radar interferometry and its application to changes in the Earth's surface. *Rev. Geophys.* 36 (4), 441–500.
- McGuinness, D.B., Hossack, J.R., 1993. The development of allochthonous salt sheets as controlled by the rates of extension, sedimentation, and salt supply. In: *Rates of Geological Processes: 14th Annual Gulf Coast Section, SEPM Foundation Bob F. Perkins Research Conference*, pp. 127–139.
- Merriam, M.F., Smoluchowski, R., Wiegand, D.A., 1962. High-temperature thermal expansion of rocksalt. *Phys. Rev.* 125.
- Rosen, P.A., Hensley, S., Peltzer, G., Simons, M., 2004. Updated repeat orbit interferometry package released. *Eos Trans. AGU* 85 (5).
- Talbot, C.J., Aftabi, P., 2004. Geology and models of salt extrusion at Qum Kuh, central Iran. *J. Geol. Soc.* 161, 321–334.
- Talbot, C.J., Jackson, M.P.A., 1987. Internal kinematics of salt diapirs. *Bull. Am. Assoc. Pet. Geol.* 71 (9), 1068–1093.
- Talbot, C.J., Pohjola, V., 2009. Subaerial salt extrusions in Iran as analogues of ice sheets, streams and glaciers. *Earth-Sci. Rev.* 97 (1–4), 155–183.
- Talbot, C.J., Rogers, E.A., 1980. Seasonal movements in a salt glacier in Iran. *Science* 208 (4442), 395–397.
- Tang, L.-J., Jia, C.-Z., Jin, Z.-J., Chen, S.-P., Pi, X.-J., Xie, H.-W., 2004. Salt tectonic evolution and hydrocarbon accumulation of Kuqa fold belt, Tarim Basin, NW China. *J. Pet. Sci. Eng.* 41, 97–108.
- Trusheim, F., 1960. Mechanism of salt migration in northern Germany. *Bull. Am. Assoc. Pet. Geol.* A 9, 1519–1540.
- Tutiempo Network, S.L., 2015. Climate KUQA – Climate Data 1956–2015. Tutiempo.net. November 2015 (updated). Accessed: December 2014, en.tutiempo.net/climate/ws-516440.html.
- Urai, J.L., Spiers, C.J., Zwart, H.J., Lister, G.S., 1986. Weakening of rock salt by water during long-term creep. *Nature* 324, 554–557.
- Walker, C.W., 1973. Nature and origin of Caprock overlying gulf coast salt domes. In: *Fourth International Symposium on Salt – Northern Ohio Geological Society*, pp. 169–195.
- Wang, X., Suppe, J., Guan, S., Hubert-Ferrari, A., Gonzalez-Mieres, R., Jia, C., 2011. Cenozoic structure and tectonic evolution of the Kuqa fold belt, southern Tianshan, China. In: McClay, K., Shaw, J.H., Suppe, J. (Eds.), *Thrust Fault-Related Folding*. In: *AAPG Mem.*, vol. 94, pp. 215–243.
- Weijermars, R., Jackson, M.P.A., Vendeville, B., 1993. Rheological and tectonic modeling of salt provinces. *Tectonophysics*, 143–174.
- Weinberg, R.F., 1993. The upward transport of inclusions in Newtonian and power-law salt diapirs. *Tectonophysics* 228, 141–150.
- Weinberger, R., Lyakhovskiy, V., Baer, G., Begin, Z.B., 2006. Mechanical modeling and InSAR measurements of Mount Sedom uplift, Dead Sea basin: implications for effective viscosity of rock salt. *Geochem. Geophys. Geosyst.* 7 (5).
- Wenkert, D., 1979. The flow of salt glaciers. *Geophys. Res. Lett.* 6 (6).
- White, D.E., 1965. Saline waters of sedimentary rocks. In: *Fluids in the Subsurface*. In: *AAPG Mem.*, vol. 4, pp. 342–366.
- Yang, S., Li, J., Wang, Q., 2010. The deformation pattern and fault rate in the Tianshan Mountains inferred from GPS observations. *Sci. China, Ser. D, Earth Sci.* 51 (8), 1064–1080.
- Yixin, Y., Pengwan, W., 2009. Balanced cross-sections of salt structures in Kuqa foreland thrust belt in northern part of Tarim basin. *J. Mar. Orig. Pet. Geol.*, 012.
- Zebker, H.A., Rosen, P.A., Goldstein, R.M., Gabriel, A., Werner, C., 1994. On the derivation of coseismic displacement fields using differential radar interferometry: the Landers earthquake. *J. Geophys. Res.* 99 (B10), 19617–19634.
- Zhao, J., Wang, J., Harbor, J.M., Liu, S., Yin, X., Wu, Y., 2015. Quaternary glaciations and glacial landform evolution in the Tailan River valley, Tianshan Range, China. *Quat. Int.* 358, 2–11.
- Zhong, D., Xia, W.S., 1998. The investigation report of Mesozoic–Cenozoic strata, structure, sedimentary facies, and petroleum potential of Kuche foreland basin outcrop area (with 1:100,000 Kuche foreland basin geologic map). Research report of Tarim Oilfield Company, Xinjiang, p. 462.
- Zubovich, A.V., Wang, X.Q., Scherba, Y.G., Schelochkov, G.G., Reilinger, R., Reigber, C., Beisenbaev, R.T., 2010. GPS velocity field for the Tien Shan and surrounding regions. *Tectonics* 29 (6).